IFS SPATIAL STRUCTURE FEATURE OF IMAGES AND ITS APPLICATIONS IN AUTOMATIC TARGET DETECTION*

ZHAO Yi-Gong ZHU Hong
(School of Electronic Engineering, Xidian University, Xi'an, Shaanxi 710071, China)

Abstract The IFS spatial structure feature was presented for detecting man-made objects in the natural background. The elementary theory of the IFS feature and the algorithm extracting the IFS feature from the practical images were both discussed in detail. Finally, some experimental results for practical infrared images were given to show the effects of the IFS feature in the automatic detection of man-made objects in the natural background.

Key words spatial structure features of images, self-affine function system, target detection.

Introduction

Fractals is a new mathematical theory used for the study of objects with complex and irregular shapes[1]. In recent years, fractals was used by researchers from different countries in the problem of detecting man-made objects in the natural background, and many significant results have been achieved[2~6]. The target detecting techniques based on fractal models and features have shown many advantages over traditional approaches and give a new promising way for automatic detection of man-made objects in the natural background. Up to now, many kinds of fractal features have been presented and were used in the research on automatic detection of man-made objects, such as fractal dimension, fractal model fitting error, spatial variation rate of geometrical measurement and so on. These fractal features are all the macro-features which describe the macro-properties of a region of an image. However, the spatial structure relationship between the whole region and the fine details of the region can not be explicitly described by them. It is believed that this kind of spatial structure relationship will be helpful in improving the ability of distinguishing man-made objects from the natural background.

IFS (Iterated Function System) is a spatial structure model which describes the spatial structure relation between the whole body and the fine part of the object concerned[7~8]. The basic idea of this paper is that, based on the IFS features of man-made

* The project supported by the Preliminary Research Foundation of National Defense
Received 1999-01-07, revised 1999-09-02

objects and the natural background, the inherent differences on IFS features between them are investigated in detail, and then the procedure detecting man-made objects in the natural background is built up according to these inherent differences.

In this paper the elementary theory of IFS is firstly overviewed. Secondly, the algorithm extracting IFS features from the practical images and how to apply IFS features to the problem of automatic detection of man-made objects in the natural background are discussed in detail. Finally, some experimental results for practical infrared images sampled in the sky, sea and ground situations are presented to show the effects of IFS features in the automatic detection of man-made objects in the natural background. .

1 Elementary Theory[7-8]

1.1 Iterated Function System-IFS

It is assumed that $\{\omega_n : X \to X, n=1,2,\ldots,N\}$ is a family of compression maps defined on a complete metric space (X,d), where X and d stand for the metric space and the distance defined on the space, respectively, and the compression ratio of ω_n is s_n. This family of compression maps is called the Iterated Function System-IFS, and its compression ratio is defined as $s=\max\{s_n; n=1,2,\ldots,N\}$.

It is defined that $W: H(X)\to H(X)$ is a map on a complete metric space $(H(X), h(d))$,

$$W(A) = \bigcup_{n=1}^{N}\omega_n(A), \quad A \in H(X), \tag{1}$$

where $H(X)\subset X$ and $h(d)$ are a family of compact sets in the space X and Hausdorff distace measure defined on the space $H(X)$ respectively, and $\{\omega_n, n=1,2,\ldots,N\}$ is an IFS with compression ratio s. It can be proved that map $W: H(X)\to H(X)$ is a compression map on the space $(H(X), h(d))$ with compression ratio s. Therefore, there exists a unique invariant set $A_f \in H(X)$ for map W, which makes

$$W(A_f) = A_f, \quad A_f \in H(X), \tag{2}$$

moreover, all series $\{W^n(A); n=1,2,\ldots\}$ will be compressed to A_f for arbitrary $A\in H(X)$

$$\lim_{n\to\infty} W^n(A) = A_f, \quad \forall A \in H(X). \tag{3}$$

Consequently, set A_f is called the abstractor of map W, or the abstractor of Iterated Function System-IFS.

The compression maps in an IFS can be defined in many forms. If they are all compressive affine transforms, the abstractor A_f of map W will have a self-affine structure, that means A_f will be a fractal set.

1.2 Collage Theorem

It can be proved that for a complete metric space (X,d) and a set $T\in H(X)$ and a constant $\varepsilon\geqslant 0$, there exists an IFS $\{\omega_n, n=1,2,\ldots,N\}$ with compression ratio $0\leqslant s<1$, which makes

$$h\left(T, \bigcup_{n=1}^{N} \omega_n(T)\right) \leq \varepsilon, \tag{4}$$

and it can also be proved that

$$h(T, A_f) \leq \frac{\varepsilon}{1-s}, \tag{5}$$

where $h(d)$ is Hausdorff distance measure and A_f is the abstractor of IFS.

An important result of Collage Theorem is that an arbitrary non-empty compact set $T \in H(X)$ in the complete metric space (X, d) can be approximated by the abstractor A_f of an IFS according to Hausdroff distance measure. Furthermore, if the compression maps $\omega_n: X \to X, n = 1, 2, \ldots, N$ in the IFS are affine transforms, then an arbitrary non-empty compact set $T \in H(X)$ can be approximated by a self-affine fractal set.

2 Computation of IFS for practical images[9]

There exist many algorithms computing IFS from an image. In this paper Bath Fractal Transform-BFT algorithm is employed for its simplicity in theory, convenience in implementation and fastness in computation.

2.1 BFT algorithm

In BFT algorithm, the compression maps in IFS are limited to self-affine transforms, in this case, the IFS becomes a Self-Affine System-SAS. In space R^2, an SAS is a family of affine transforms as follows.

$$w_k(x, y) = \begin{bmatrix} a_{11}^{(k)} & a_{12}^{(k)} \\ a_{21}^{(k)} & a_{22}^{(k)} \end{bmatrix} \begin{bmatrix} x \\ y \end{bmatrix} \begin{bmatrix} b_1^{(k)} \\ b_2^{(k)} \end{bmatrix}, \quad (k = 1, 2, \ldots, N). \tag{6}$$

A practical image is a gray-level function $g(x, y), (x, y) \in R^2$, which is defined on a region A of R^2 plane. For the defining region A of an image it is possilbe to choose an SAS so that its abstractor is the same as the defining region of the image

$$A = \bigcup_{i=1}^{N} \omega_i(A). \tag{7}$$

Figure 1 intuitively shows the relationship between the rectangular defining region of a practical image and a fourth-order SAS. From Fig. 1 it can be seen that the abstractor of the SAS is a non-overlap overlay of the defining region of the image, and the shape of the abstractor of the SAS is completely the same as that of the defining region of the image. Therefore, a precise self-affine relation exists between the whole body and local part of the defining region of the image.

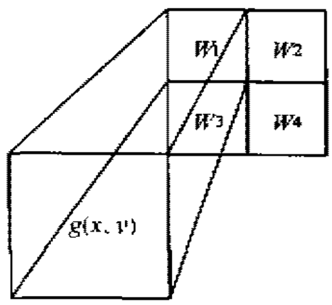

图 1

Fig. 1 Domain of image and corresponding SAS

图 1　图像域及相应的 SAS

A practical image is a gray-level function on its defining region. It is hoped that a similar self-affine relation also exists between the whole body image gray-level function $g(x, y)$ and the local part image gray-level function $g(w_k(x,y))$, namely

$$v_k(x,y,g(x,y)) = a^{(k)} - b_1^{(k)}x - b_2^{(k)}y + c^{(k)}g(x,y), \quad \forall (x,y) \in A. \tag{8}$$

It can be proved that Eq. (8) is true for a fractal image, and not true for a non-fractal image, so for a non-fractal image, the transfrom $v_k(\cdot)$ can be determined only in the sense of function approximation.

It is assumed that after transforming the whole body image $g(x,y)$ with transfrom $v_k(\cdot)$, an image block $g'(w_k(x,y))$ will be obtained which is an approximation to the true local image block $g(w_k(x,y))$. With the criterion of root-mean-square, we have

$$e_{rms}^{(k)} = \int_{(x,y)\in A}[g(w_k(x,y)) - g'(w_k(x,y))]^2 dL$$
$$= \int_{(x,y)\in A}[g(w_k(x,y)) - a^{(k)} - b_1^{(k)}x - b_2^{(k)}y - c^{(k)}g(x,y)]^2 dL \tag{9}$$

where A is the defining region of the image, L is the Lebesgue measure on space R^2. If the approximation error between $g'(w_k(x,y))$ and $g(w_k(x,y))$ is minimized, we have

$$\frac{\partial e_{rms}^{(k)}}{\partial a^{(k)}} = \frac{\partial e_{rms}^{(k)}}{\partial b_1^{(k)}} = \frac{\partial e_{rms}^{(k)}}{\partial b_2^{(k)}} = \frac{\partial e_{rms}^{(k)}}{\partial c^{(k)}} = 0 \tag{10}$$

Consequently, a group of linear equations can be obtained from Eqs. (8), (9) and (10)

$$\begin{bmatrix} \int x^2 & \int xy & \int xg(x,y) & \int x \\ \int xy & \int y^2 & \int yg(x,y) & \int y \\ \int xg(x,y) & \int yg(x,y) & \int [g(x,y)]^2 & \int g(x,y) \\ \int x & \int y & \int g(x,y) & \int 1 \end{bmatrix} \begin{bmatrix} b_1^{(k)} \\ b_2^{(k)} \\ c^{(k)} \\ a^{(k)} \end{bmatrix} = \begin{bmatrix} \int xg[w_k(x,y)] \\ \int yg[w_k(x,y)] \\ \int g(x,y)g[w_k(x,y)] \\ \int g[w_k(x,y)] \end{bmatrix} \tag{11}$$

where the integral regions are all the defining region A of the image. From this group of linear equations, four coefficients $a^{(k)}$, $b_1^{(k)}$, $b_2^{(k)}$ and $c^{(k)}$ can be obtained, that means each block of the non-overlap overlay of the image can be described by these four coefficients.

2.2 Application of BFT algorithm in detection of man-made objects in the natural background

From what mentioned above it is known that if an image has a fractal structure itself, i.e. there exists a self-affine relation between the whole body and the local part of the image, and the transforms v_k are limited within affine transforms, then the approximation error e_{rms} will be very small, theoretically equals zero; otherwise if the image does not have a fractal structure, the approximation error e_{rms} will be very large. Based on this fact it can be determined according to the approximation error whether the image concerned has a fractal structure. By many results of theoretical research and analysis of practical data, it has been convinced that the images of various natural backgrounds accord with the fractal models, whereas the images of the man-made objects do not accord with the fractal models. Therefore, the man-made objects in the natural background can be detected according to the value of approximation error e_{min}.

In the practical applications of approximating an image block by BFT transform, the approximation can be investigated between adjacent image blocks, and it is unnecessary to limit the approximation investigation only within an image block. For the man-made objects in the natural background, since the objects are surrounded by the background and in view of the fact that the backgrounds accord with the fractal models and the objects do not, whether the object image block is to be approximated by the adjacent background image blocks or the adjacent background image blocks are to be approximated by the object image block, large approximation error will all arise in both cases. Based on this fact, the procedure detecting man-made objects in the natural background in this paper is composed of two steps: firstly, the BFT approximation error image is obtained by computing the BFT approximation error between adjacent image blocks, and then the man-made objects in the natural background are detected according to the approximation errors.

3 Experiment results

By means of the target detetion technique based on the IFS features, many experimental results have been obtained for the infrared images sampled in the practical sky, sea and ground situations. Some of them are shown in Figs. 2 ~ 4.

Experiment parameters are: image size = 256 × 256 pixel². Since the procedure of automatic target capturing is mainly used for the small targets with size less than 20 × 20 pixel² in practical situations, the size of image blocks is chosen as 8 × 8 pixel².

(a)　　(b)　　(c)

Fig. 2　BFT feature extracted for an airplane in the sky. (a) original image, (b) image of BFT approximating error, (c) result obtained by image segmentation

图 2　空中飞机 BFT 特征提取的结果

(a) 原始图像，(b) BFT 逼近误差分布图像，(c) 图像分割检测的结果

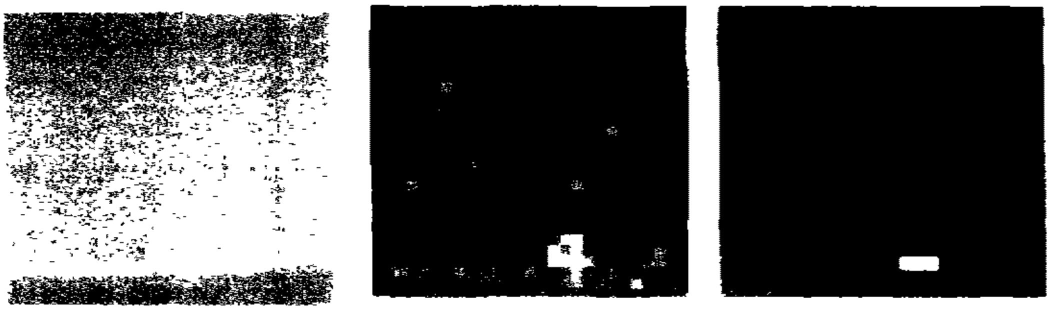

(a) (b) (c)

Fig. 3 BFT feature extracted for a ship on the sea. (a) original image, (b) image of BFT approximating error, (c) result obtained by image segmentation.

图3 海面舰船BFT特征提取的结果

(a)原始图像,(b)BFT逼近误差分布图像,(c)图像分割检测的结果

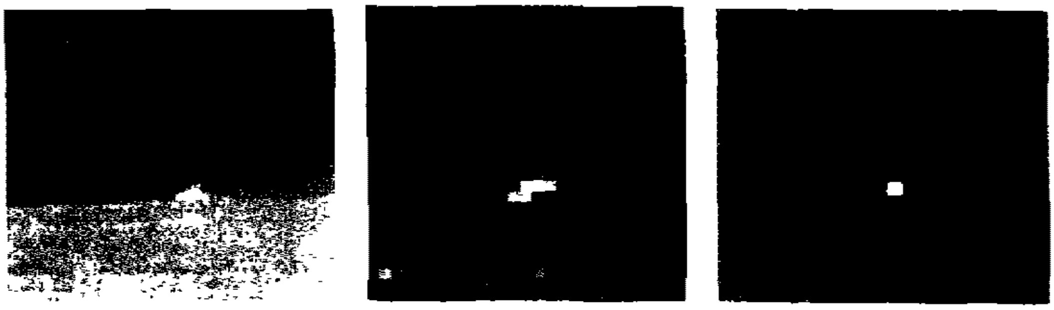

(a) (b) (c)

Fig. 4 BFT feature extracted for a tank on the ground. (a) original image, (b) image of BFT approximating error, (c) result obtained by image segmentation

图4 地面坦克BFT特征提取的结果

(a)原始图像,(b)BFT逼近误差分布图像,(c)图像分割检测的结果

In the simulation experiment, the image of BFT approximation error is obtained by computing the BFT approximation error between a certain local image block and four local image blocks adjacent to it, then a segmenting threshold is computed according to the image of approximation error, finally the man-made objects can be segmented from the natural background by use of the threshold.

It can be seen from the experimental results that the contrast between the targets and background has been significantly enhanced in the images of BFT approximating error. As a result, the ability distinguishing man-made objects from natural background has been improved.

REFERENCES

1 Mandelbrot B B. *The Fractal Geometry of Nature*, San Francisco: Freeman, 1982

2 Stein M C. Fractal image models and object detection, *Visual Comm. and Image Proc.* Ⅱ, *SPIE*,

1987, **845**: 293～300

3 Peli T. Multiscale fractal theory and object characterization. *J. Opt. Soc. Am. A*, 1990, **7**(6): 1101～1112.

4 ZHAO Yi-Gong, ZHU Hong. Adaptive detection of man-made objects in natural background. *Acta Electronica Sinica* (赵亦工，朱　红．自然背景中人造目标的自适应检测，**电子学报**), 1996, **24**(4): 17～20

5 ZHAO Yi-Gong, ZHU Hong. Detection of man-made objects by fractal models. *J. Infrared Millim. Waves* (赵亦工，朱　红．基于分形模型的人造目标检测技术，**红外与毫米波学报**), 1995, **14**(5): 336～340

6 ZHAO Yi-Gong, ZHU Hong. A new feature based on fractal models and its applications in automatic target recognition. *J. Infrared Millim. Waves* (赵亦工，朱　红．一种基于分形模型的新特征及其在自动目标识别中的应用，**红外与毫米波学报**), 1997, **16**(3): 217～220

7 Barnsley M F. *Fractal Everywhere*. Boston: Academic Press, 1988

8 Barnsley M F. *Fractal Image Compression*. Massachusetts: AK Peters Ltd. Wellesley, 1993

9 Monro D M, Dudbridge F. Fractal approximation of image blocks. *ICASSP92*, Vol. Ⅲ, March 1992, 485～488

IFS 图像空间结构特征及自动目标检测*

赵亦工　朱　红

（西安电子科技大学电子工程学院，陕西，西安，710071）

摘要　一个迭代函数系（IFS（Iterated Function System））由一组压缩映射组成，它描述了研究对象"整体"和"局部"之间的变换构成关系。对于图像来讲，IFS 描述了图像"整体"和"局部"之间的空间变换关系，因此，IFS 可以成为图像的空间结构模型，而与 IFS 有关的参数可以视为反映图像空间结构的特征。

IFS 的提出起源于分形图像压缩的研究，因此 IFS 与分形之间存在着密切的和内在的联系。IFS 的理论中有两个重要的结论：一是如果 IFS 中的压缩映射均为仿射变换，则 IFS 的吸引子将是一个分形集合；二是实际中所遇到的图像都可以用 IFS 的吸引子逼近。根据这两个结论，如果限定 IFS 中的压缩变换均为仿射变换，又图像本身具有分形结构，即图像"整体"和"细节"之间存在仿射变换关系，则用 IFS 的吸引子逼近图像时产生的误差很小（理论误差值为 0）；如果图像本身不具有分形结构，则逼近误差很大。所以，根据 IFS 逼近误差的大小，即可判定被研究的图像是否具有分形结构特征。大量的理论研究和实验数据分析表明，自然背景的图像符合分形模型，而人造目标的图像不符合分形模型。因此，可以根据 IFS 逼近误差的大小实现对自然背景中人造目标的检测。

提取图像 IFS 的算法有多种，本文采用 Bath Fractal Transform（BFT）算法，它是一个原理简单、实现方便、运算速度快的算法。该算法可以研究图像块自身或不同图像块之间"整体"与"局部"之间的空间结构关系。

对于自然背景中的人造目标，由于目标被自然背景包围，因此，不论是用邻近目标的背景图像块逼近目标图像块，还是用目标图像块逼近邻近的背景图像块，都会产生较大的逼近误差。根据这一结论，本文在研究自然背景中人造目标的检测过程中，通过计算邻近图像块之间的 BFT 逼近误差，获得逼近误差图像，进而根据逼近误差检测自然背景中的人造目标。

实际数据仿真实验的结果证实了本文所提方法的有效性。

关键词　图像空间结构特征，自仿射函数系，目标检测。

* 国防科技预研基金（编号：95J2.3.1）资助项目

稿件收到日期 1999-01-07，修改稿收到日期 1999-09-02